Recent imaging modalities in the diagnosis of peritoneal carcinomatosis

Essay

Submitted for partial fulfillment of Master Degree in **Radio-diagnosis**

Presented by

Dr.Ehab Abdel Hamid Diab M. B. B. Ch

Supervised by

Prof. Dr. Nabil Yousef Khattar

Professor of Radio-diagnosis Faculty of Medicine-Cairo University

Prof. Dr. Maha Helal

Professor of Radio-diagnosis National Cancer Institute-Cairo University

> Faculty of Medicine Cairo University 2012

(بسم الله الرحمن الرحيم) قالم اسبحانك لاعلم لذا الا ماعلمتذا اذك اذت العليم الحكيم

البقره: ٣٢ (صدق الله العظيم)

ACKNOWLEDGEMENT

First and foremost, I'm always indebted to **ALLAH**, the most kind and merciful.

I would like to express my deepest and greatest respect to Professor Dr. Nabil Khattar, Professor of diagnostic radiology, Cairo University, I had the honor to proceed with this work under his supervision, for his invaluable knowledge, kind guidance and continuous support that I will always be grateful for.

I would like to express my deepest appreciation and cordial thanks to Professor Dr. Maha Helal, Professor of diagnostic radiology, National Cancer Institute, for her persistent effort, guidance and meticulous revision of this work.

Finally, I would like to express my warmest appreciation and sincere gratitude to my family for their endless love and support.

Abstract

As surgical and chemotherapeutic strategies in peritoneal carcinomatosis evolve, imaging needs to provide better resolution over the entire peritoneal surface in order to identify small implants and diffuse disease.

Conventional imaging as MDCT and MRI of peritoneal carcinomatosis has a satisfactory performance in most patients

MDCT with Multi Planar Reformating demonstrates the size and location of peritoneal implants. It has a sensitivity of 85–93% and a specificity of 82%. The advantages of CT in peritoneal carcinomatosis detection are wide availability, good reproducibility, high cost-efficiency and fast scanning times but it is ionizing radiation, suboptimal sensitivity in sub centimeter lesions and certain anatomical locations.

Key Words:

Gradient echo - Computed tomography - Fluro-2-deoxy-d-glucose.

Contents

-Chapter I: Introduction and aim of the work6
-Chapter II: Anatomy of the peritoneum9
-Chapter III: Pathology of peritoneal carcinomatosis25
-Chapter IV: MDCT imaging of peritoneal carcinomatosis39
-Chapter V: PET/CT imaging of peritoneal carcinomatosis55
-Chapter VI: MR imaging of peritoneal carcinomatosis68
-Chapter VII: Diffusion weighted MR imaging of peritoneal carcinomatosis80
-Chapter VIII: Ultrasound of peritoneal carcinomatosis97
-Chapter IX: Discussion ,Summary and Conclusion110
- References119
- Arabic Summary130

LIST OF FIGURES

Fig. 1: Visceral peritoneum	10
Fig. 2: The intra and retroperitoneal structure	
Fig. 3: The initia and retroperitorieal structure	
Fig. 4: Median section through the abdomen to show the peritoneal cavity	
Fig. 5: The greater omentum	
Fig.6: The mesentery	
Fig.7: The transverse mesocolon	
Fig.8: The falciform ligament	
Fig.9: The site of bare area of the liver	
Fig.10: The gastrohepatic ligament	
Fig.11: The hepatoduodenal ligament anatomic cross section	
Fig.12: The phrenicocolic ligament frontal	
Fig.13: The gastrosplenic ligament	
Fig.14: Horizontal sections through the abdomen	
-	
Fig.15: Sagittal schemes of the greater omentum	
Fig. 13: Nodel mass within postuply agatic ligament	
Fig.17: Nodal mass within gastrohepatic ligament	
Fig.18: Tumor infiltrate hepatoduodenal ligament	
Fig.19: Extension of gastric carcinoma along the gastrocolic ligament	
Fig.20: Spread of pancreatic carcinoma into transverse mesocolon	
Fig.21: Spread of carcinoma of right colon across duodeno-colic ligament	
Fig.22: Spread of gastric carcinoma across gastrosplenic ligament to spleen	
Fig.23: Spread of gastric carcinoma to gastrosplenic and splenorenal ligaments	
Fig.24: Spread of pancreatic carcinoma into phrenicocolic ligament	
Fig.25: Fifty-nine-year-old woman with carcinoma of the head of the pancreas	
Fig.26: Carcinoid tumor with mesenteric metastases	
Fig.27: Malignant GIST with mesenteric metastases	
Fig.28: Illustration shows the pathways of flow of intraperitoneal fluid	
Fig.29: C.T image show the sandwich sign	
Fig.30: Metastatic melanoma in a 50-year-old	
Fig.31: Different aspects of peritoneal implants	
Fig. 32: Micronodular pattern	
Fig.33: A stellate nodule over ascending colon	
Fig.34: Omental Cake	
Fig.35: "Plaque like" implant	
Fig.36: "Mass like" implant	
Fig.37: Teca Aspect	
Fig.38: Peritoneal carcinomatosis from adenocarcinoma of the colon	
Fig.39: Diaphragmatic implant in a patient with ovarian cancer	
Fig.40: Diaphragmatic implant in a patient with newly diagnosis of ovarian cancer	
Fig.41: Tumor scalloping of liver surface in a patient with ovarian cancer	
Fig.42: Splenic implants in a patient with ovarian cancer	
Fig.43: Porta hepatis implants in a woman with ovarian cancer	
Fig.44: Peritoneal metastases in the paracolic gatters	
Fig.45: Omental caking in a woman with ovarian cancer abdomino-pelvic CT	
Fig.46: Necrotic bowel implant in a woman with ovarian cancer	
Fig.47: Vaginal cuff implants in a patient with history of ovarian cancer and hysterectomy	
Fig.48: Relationship of a primary ovarian mass to the pelvic vessels	
Fig.49: Diffuse peritoneal metastases from ovarian cancer	53

Fig.50: Photograph (side view) of a hybrid PET-CT scanner	
Fig.51: Typical scout obtained during an FDG PET-CT study	
Fig.52: Normal FDG uptake	
Fig.53: Hypermetabolic activity of omental cake	
Fig.54: Postoperative PET/CT of a patient with peritoneal carcinomatosis	61
Fig.55: PET/CT image of mixed solid and cystic lesion	
Fig.56: PET/CT image shows hypermetabolic activity in solid components of masses	62
Fig.57: Tumor implants in a 59 years old woman	63
Fig.58: Tumor implants in a 59 years old woman	
Fig.59: Tumor implants in a 55-year-old woman with ovarian cancer	64
Fig.60: Midabdominal tumor in a woman with a history of serous ovarian cancer	
Fig.61: Physiologic FDG activity in bowel loops in a patient	
Fig.62: Misregistration artifact	
Fig.63: Non-neoplastic hypermetabolic activity	
Fig.64: PET-CT scan shows a uterine fibroid with no FDG activity	
Fig.65: The response of a gastrointestinal stromal tumor to chemotherapy	
Fig.66: Diffuse increase in bone marrow activity following chemotherapy	
Fig.67: Increased FDG activity around hip replacement	
Fig.68: Physiologic FDG activity in bowel loops in a patient	
Fig.69: Periportal gastric cancer spread	
Fig.70: Nodular enhancement of peritoneum	
Fig.71: Treated ovarian cancer with recurrence	
Fig.72: Implant perihepatic peritoneal tumor	
Fig.73: Mesenteric tumor in patient with ovarian cancer	
Fig.74: Omental tumor	
Fig.75: Serosal tumor	
Fig.76: Parietal peritoneal tumor	
Fig.77: Sigmoid peritoneal tumor	
Fig.78: Peritoneal carcinomatosis in a female patient with stage III ovarian cancer	
Fig.79: Residual peritoneal tumor in a patient underwent primary debulking surgery	
Fig.80: Residual peritoneal tumor in a patient underwent primary debulking surgery	
Fig.81: Omental cake in a female patient with primary peritoneal cancer	
Fig.82: Postoperative changes in a patient with stage II A ovarian cancer	
Fig.83: Recurrent ovarian cancer	
Fig.84: Metastatic well differentiated serous carcinoma of the ovary	
Fig.85: Metastatic well differentiated carcinoma of the ovary	
Fig.86: Abdominal abscess in a female patient with stage III ovarian cancer	
Fig.87: Ovarian cyst and normal endometrium	
Fig. 88: Optimization of ultrasound technique	
Fig. 89: Normal appearance of the mesentery surrounded by ascites	
Fig. 91: Calcified implemes in a patient with parents appearing page 19.	
Fig. 93: Calcified implants in a patient with serous ovarian neoplasm	
Fig.92: Peritoneal carcinomatosis in a patient without ascites	
Fig.94: Omental cake in male patient	
Fig.95: Omental cake in a woman with proved metastatic adenocarcinoma	
Fig.96: Mesenteric tumor deposits in a patient metastatic hepatocellular carcinoma	
Fig.97: Quantification of ascites in a patient with liver cirrhosis and portal hypertension	
Fig.98: Quantification of ascites in a patient with ovarian cystadenocarcinoma	
Fig.99: Characterization of peritoneal fluid CT and ultrasound images	
116.55. Characterization of peritorical hala er and altrasound images	103
Table.9.1: Comparison between sensitivity, specificity, advantage and disadvantage	115

List of abbreviation

ADC: Apparent diffusion coefficient

DWMRI: Diffusion weighted magnetic resonance imaging.

CT: Computed tomography.

FDG: Fluro-2-deoxy-d-glucose.

GE: Gradient echo.

FLAIR: Fluid attenuation inversion recovery.

MPR: Multi planar reformatted.

MR: Magnetic resonance.

MRI: Magnetic resonance imaging.

PET: Positron emission tomography.

PET/CT: Fused Positron emission tomography and Computed tomography.

RARE: Rapid acquisition with relaxation enhancement.

SUV: Standardized uptake value.

Chapter I Introduction & Aim of work

Peritoneal Carcinomatosis is defined as seeding and implantation of neoplastic cells into the peritoneal cavity and it may represent the advanced stage of every tumors developed into the abdominal and pelvic organs. However ovarian, stomach and colorectal cancers accounts for almost all cases. (*Ciolina et al.*, 2012)

Traditionally, the peritoneal carcinomatosis has been considered as a late incurable stage of the neoplastic injury, subsidiary of palliative systemic chemotherapy only, with or without reduction surgery of the tumoral mass (debulking). (Levy et al., 2008)

However, the studies carried out in the 1980s suggested that peritoneal carcinomatosis should be faced as a locoregional stage, and that a limited peritoneal seeding can be cured (40% in gastrointestinal origin cases) using a combination of debulking surgery and intraperitoneal perioperative chemotherapy. Evaluating the extent of disease critically determines tumor resectability and can also predict outcome (*Kyriazi et al.*, 2010b).

Peritoneal imaging is a challenge for most radiological studies. The extensive nature of the peritoneum makes it a difficult organ to visualize. In addition, peritoneal tumors can be subtle, although, widely disseminated. Plain radiographs and barium examinations have little value in patients with peritoneal tumor, until tumors are so large that they deform the barium column (*Low et al.*, 2007).

Most CT scan findings are however nonspecific as both neoplastic and non-neoplastic pathologies of the peritoneum present as soft-tissue masses, with or without ascites. In addition, there may also be a cystic component, necrosis, calcification, or significant contrast enhancement. Sometimes, peritoneal nodules can simulate unopacified bowel loops and hence adequate bowel opacification is important for accurate diagnosis. The CT appearance of

neoplastic infiltration of the greater omentum can range from increased density of fat anterior to the colon or small bowel, to large masses, called omental cakes, separating the colon and small bowel from the anterior abdominal wall (smiti et al., 2010).

However, detection of subcentimeter deposits provides vital prognostic information since the presence of residual foci as small as 5 mm is an adverse prognostic factor (*Chi et al.*, 2006).

In addition to size, the anatomical location determines whether the lesions can be detected, particularly in the absence of ascites; the right subdiaphragmatic space, omentum, root of mesentery and serosal surface of the small bowel frequently harbor occult tumors and are associated with a CT sensitivity of 11–37%, (*Coakley et al.*, 2002).

Functional imaging techniques, such as PET/CT and diffusion-weighted MRI have an emerging role in detection of the peritoneal deposits, staging of the primary tumor and assessing treatment response. The combination of functional information with conventional anatomical visualization holds promise to accurately characterize peritoneal disease, and provides non-invasive biomarkers of therapeutic performance and patient prognosis (*Kyriazi et al.*, 2010b).

The aim of this study is to evaluate the different recent imaging modalities in the diagnosis and prognosis of peritoneal metastases with highlights on the standard conventional techniques.

Chapter II Anatomy of The Peritoneum

The peritoneum is the largest serous membrane of the body; it consists of a layer of simple squamous epithelium (mesothelium) with an underlying supporting layer of areolar connective tissue. The peritoneum is divided into:

The parietal peritoneum, which lines the wall of the abdomino-pelvic cavity.

The visceral peritoneum, which covers some of the organs in the cavity.

(Tortora& Derrickson., 2000)

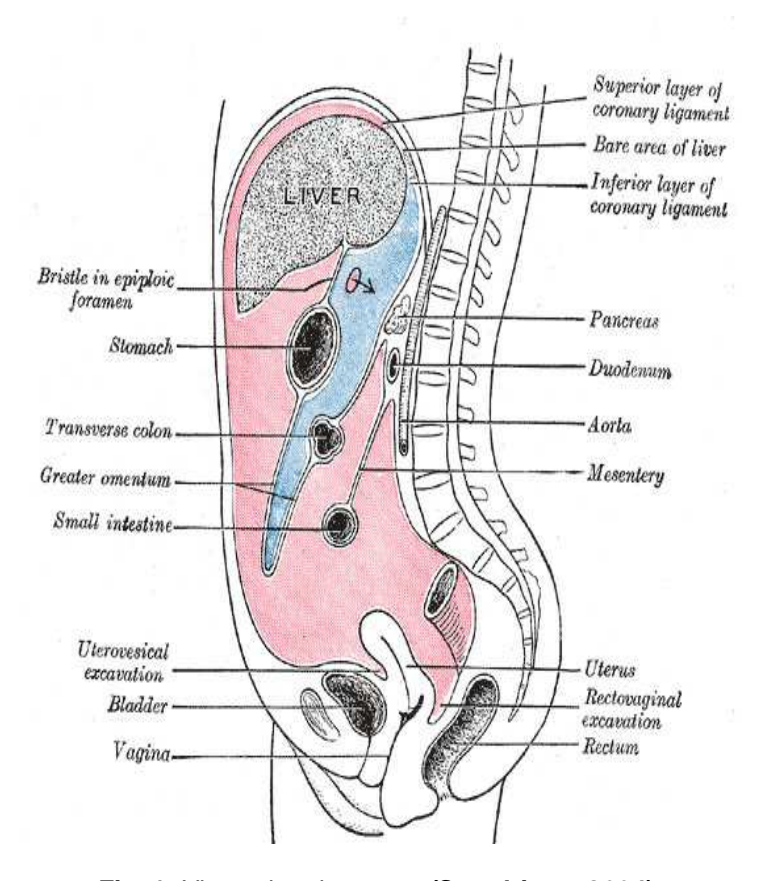


Fig. 1: Visceral peritoneum. (Standring ., 2004).

The slim space containing lubricating serous fluid between the parietal and visceral portions of the peritoneum is called the **peritoneal cavity.** In certain diseases, the peritoneal cavity may become distended by the accumulation of several liters of fluid, a condition called **ascites.**Unlike the pericardium and pleurae, which smoothly cover the heart and lungs, the peritoneum contains large folds that weave

between the viscera. The folds bind the organs to one another and to the walls of the abdominal cavity. They also contain blood vessels, lymphatic vessels, and nerves that supply the abdominal organs (fig.1) (*Tortora& Derrickson.*, 2000)

Function of the peritoneum

- Secretes a lubricating serous fluid that continuously moistens the associated organs and allows free movement of the abdominal viscera
- Its fluid content minimizes friction and resists infection.
- In response to injury or infection (peritonitis), it exudes fluid and cells and tends to wall off or localize infection. (O'Rahilly & Muller., 1983)

The relationship between the viscera and the peritoneum

<u>Intraperitoneal viscera</u>: completely surrounded by peritoneum, examples: stomach, superior part of duodenum, jejunum, ileum, cecum, vermiform appendix, transverse and sigmoid colons, spleen and ovaries (fig.2).

<u>Interperitoneal viscera</u>: most parts of viscera are surrounded by peritoneum, examples: liver, gallbladder, ascending and descending colon, upper part of rectum, urinary bladder and uterus (fig.2).

Retroperitoneal viscera: some organs lie on the posterior abdominal wall and are covered by peritoneum on their anterior surfaces only, example: kidney, suprarenal gland, pancreas, descending and horizontal parts of duodenum, middle and lower parts of the rectum, and the ureters (fig.2). (*Tortora& Derrickson.*, 2000)

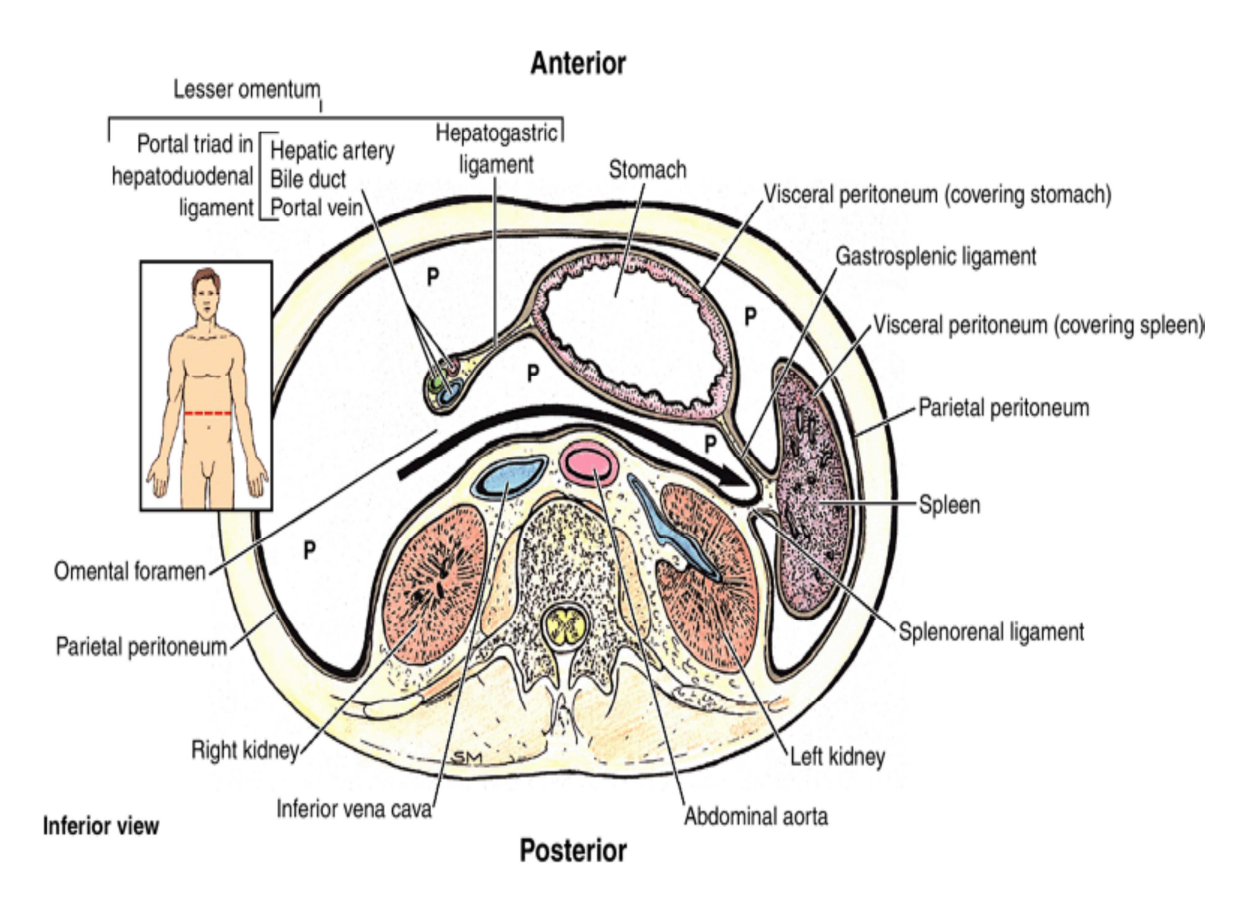


Fig. 2: The intra and retroperitoneal structures. (*Tortora& Derrickson.*, 2000)

Structures formed by the peritoneum

Omentum

Two-layered fold of peritoneum that extends from stomach to adjacent organ.

<u>Lesser omentum</u> two-layered fold of peritoneum which extends from porta hepatis to lesser curvature of stomach and superior part of duodenum

- **Hepatogastric ligament:** extends from porta hepatis to lesser curvature of stomach
- -Hepatoduodenal ligament: extends from porta hepatis to superior part of duodenum. Contains common bile duct, hepatic artery and portal vein. (*Tortora& Derrickson.*, 2000)